american physiological society

JNP JOURNAL OF NEUROPHYSIOLOGY

J Neurophysiol 129: 431–444, 2023.
First published January 4, 2023; doi:10.1152/jn.00449.2022

RESEARCH ARTICLE

Sensory Processing

Odor encoding by signals in the olfactory bulb

Justus V. Verhagen,[1,2] Keeley L. Baker,[1,2] Ganesh Vasan,[1,2] Vincent A. Pieribone,[1,2,3] and Edmund T. Rolls[4,5]

[1]*The John B. Pierce Laboratory, New Haven, Connecticut;* [2]*Department of Neuroscience, Yale University, New Haven, Connecticut;* [3]*Department of Cellular and Molecular Physiology, Yale School of Medicine, New Haven, Connecticut;* [4]*Oxford Centre for Computational Neuroscience, Oxford, United Kingdom; and* [5]*University of Warwick, Coventry, United Kingdom*

Abstract

To understand the operation of the olfactory system, it is essential to know how information is encoded in the olfactory bulb. We applied Shannon information theoretic methods to address this, with signals from up to 57 glomeruli simultaneously optically imaged from presynaptic inputs in glomeruli in the mouse dorsal (dOB) and lateral (lOB) olfactory bulb, in response to six exemplar pure chemical odors. We discovered that, first, the tuning of these signals from glomeruli to a set of odors is remarkably broad, with a mean sparseness of 0.83 and a mean signal correlation of 0.64. Second, both of these factors contribute to the low information that is available from the responses of even populations of many tens of glomeruli, which was only 1.35 bits across 33 glomeruli on average, compared with the 2.58 bits required to perfectly encode these six odors. Third, although there is considerable interest in the possibility of temporal encoding of stimulus including odor identity, the amount of information in the temporal aspects of the presynaptic glomerular responses was low (mean 0.11 bits) and, importantly, was redundant with respect to the information available from the rates. Fourth, the information from simultaneously recorded glomeruli asymptotes very gradually and nonlinearly, showing that glomeruli do not have independent responses. Fifth, the information from a population became available quite rapidly, within 100 ms of sniff onset, and the peak of the glomerular response was at 200 ms. Sixth, the information from the lOB was not additive with that of the dOB.

NEW & NOTEWORTHY We report broad tuning and low odor information available across the lateral and dorsal bulb populations of glomeruli. Even though response latencies can be significantly predictive of stimulus identity, such contained very little information and none that was not redundant with information based on rate coding alone. Last, in line with the emerging notion of the important role of earliest stages of responses ("primacy"), we report a very rapid rise in information after each inhalation.

information encoding; mouse; olfactory bulb; rate encoding; temporal encoding

INTRODUCTION

There are ~1,000 types of glomeruli in the rodent olfactory bulb (OB), each receiving input from thousands of olfactory receptor neurons (ORNs) expressing only 1 of the >1,000 gene-specified olfactory receptors (1–3). Pre- and postsynaptic neurons in some of the glomeruli appear to be quite tuned to, for example, odors with particular carbon-chain lengths (3–6). In particular, when presented at relatively low (pM to nM) concentrations, tuning was very sparse (7). Inhibitory action by "natural" odorant mixture components on ORNs may sharpen tuning to mixtures (8). On the other hand, broad tuning has also been reported with flow dilutions around 0.1–10% of saturated vapor pressure (9–11), as well as odor concentration-dependent glomerular recruitment (11–14). However, there has been, as far as we know, no previous information theoretic quantification of how populations of glomeruli encode a set of typical monomolecular olfactory stimuli. There are a whole set of key questions, which we aimed to investigate.

First, can a subset of glomeruli perfectly encode each of a set of typical odors? Or are more than a subset needed, which might be consistent with mammals utilizing ~1/30th of their genome to code for olfactory receptors, which itself is a

Correspondence: J. V. Verhagen (jverhagen@jbpierce.org); E. T. Rolls (Edmund.Rolls@oxcns.org).
Submitted 15 November 2022 / Revised 21 December 2022 / Accepted 22 December 2022

strikingly large proportion of the genome? Second, how independent is the coding by different glomeruli to a set of typical odors: does the information from different glomeruli add up linearly, indicating independent encoding? Third, how much information is there in the firing rates of the glomeruli, and how much information is temporally encoded by the latency of the response of each glomerulus to an odor? Moreover, do these two types of information add, or is any information in the latencies redundant with respect to the information in the rates? Fourth, how long does it take for the information about which stimulus was presented to become available from the responses of the glomeruli?

The only way that we know to address questions of this type is to use Shannon information theory. Shannon information theory (15) provides a principled approach to this type of question, because information measures are additive if they are independent; and the amounts of information from different measures can be directly compared, including for example neuronal, functional (f)MRI, and behavioral measures (16–20). In the research described here, we therefore used Shannon information theory to measure the encoding of a set of odors by glomeruli in the mouse dorsal and lateral olfactory bulb. The set of six odors used was heptanone, hexanal, amyl acetate (AA), carvone, methyl valerate (MV), and heptanol. These odors were chosen to represent different molecular groups, as well as to be represented in the dorsal and lateral bulb (10, 21–23). The responses of the glomeruli were measured with optical calcium imaging in anesthetized mice, and their general spatial and temporal properties have been described previously (10). The signal obtained with this method reflects the firing rates of the neurons in a glomerulus (24, 25).

Part of the importance of this research is that there has been great interest in whether temporal encoding, for example response latency, is important in neural encoding in the olfactory system. The dynamic glomerular activation patterns unfold over ~200 ms across the dorsal glomerular layer after inhalation during odor presentation (26). Mice can discriminate glomerular input activity duration differences down to only 10 ms (27) and detect temporal odor information down to 10 ms relative to the sniff cycle (28). Furthermore, mice are able to discriminate the temporal differences in optogenetic activation of spatially separated glomeruli across the dorsal bulb of only 13 ms, independently of sniff timing (29).

In addition, odorants present in a turbulent plume can be both spatially and temporarily sparse (30). It appears, however, that a subset of mitral/tufted cells are able to closely track the temporal structure thereof (31–35) and that mice are able to discriminate fluctuations up to 40 Hz (34). They furthermore can robustly navigate to the source of such odor plumes based on odor alone (36) or ultimately also on learned source options (37). This temporal sparseness exists in the biological reality of active sampling, which at best exposes odors to the epithelium for a fraction of a second (38).

In fact, some behavioral decisions occur well before the glomerular olfactory receptor neuron (ORN) responses in the rodent olfactory bulb (OB) reach peak amplitude. The early responses of only a subset of glomeruli may be sufficient for accurate decisions, a phenomenon termed "primacy" (39). It remains unclear, however, how rapidly information becomes available about an odorant set over time and over an increasing number of glomeruli. It also remains unknown as to how much information is represented about stimuli by way of response dynamics. To quantify the information across response time, glomeruli, and glomerular dynamics, we used information theory and new approaches developed from those that we introduced previously (40, 41).

The data set used for the analyses described here are the spatiotemporal responses of presynaptic glomeruli (i.e., terminals of ORNs) from simultaneously optically imaged OMP-GCaMP6f mouse dorsal and lateral OB (10). We used this data set to quantify information about which stimulus was presented and how the information was represented. The magnitudes of the responses termed "Rates" were estimated by deconvolving optically imaged calcium responses with 140-ms decay times, based on evidence of the relation between spike rates and the calcium signal from visual cortex in mice (25).

METHODS

The acquisition of the data analyzed here has been described previously (10). Full methods of acquiring glomerular odor responses can be found there. An abbreviated version of the most salient aspects is provided below, followed by a description of how the data were prepared for the information theoretic analyses described here. Whereas in Baker et al. (10) the analysis was primarily on the first odor responses during a trial at two concentrations, here we analyzed data from the first five sniff responses each time an odor was delivered at 1% of saturated vapor (% s.v.). The focus here was on the analysis of information encoding of odor quality rather than effects of odor intensity in the olfactory bulb, and the information theoretic methods used are described below.

Surgery

Five *OMP-GCaMP6f* mice [generated by crossing *OMP-Cre* (Jax Stock No. 006668) with *GCaMP6f* floxed transgenic mice (Jax Stock No. 024105)] aged 12–20 wk, both males and females, were used. They were anesthetized with isoflurane (4% for induction, 1.5–2.5% for maintenance). Anesthetic maintenance was monitored by the pedal withdrawal reflex and supplemented as needed. Core body temperature of the animal was maintained at ~37°C with a thermostatically controlled heating pad. After surgery, the animals were placed in their home cage on a heating pad. Carprofen (5 mg/kg sc) was administered before surgery and buprenorphine (50 μg/kg im) at the start of surgery. Mice received supplemental carprofen 24 h after surgery, and weight was monitored for the duration of the experiment. Animals were placed in a stereotaxic holder and prepared by aseptic procedures. For exposure of the dorsal olfactory bulb, the skin was removed and the underlying bone was thinned with a dental drill. For exposure of the lateral olfactory bulb, an enucleation of the left eye was performed and the upper and lower eyelids were removed. The bone overlying the lateral portion of the olfactory bulb was thinned. A seamless covering of cyanoacrylate was applied to both the dorsal and lateral windows at once. A head cap was secured with cyanoacrylate and dental cement for stability during imaging. Animals were given at least 24 h of recovery after surgery before imaging to reduce any OB inflammation as a result of windowing. All procedures were performed in accordance with

protocols approved by the Pierce Animal Care and Use Committee (PACUC). These procedures are in agreement with the National Institutes of Health *Guide for the Care and Use of Laboratory Animals* (8th ed.).

Imaging

All imaging was carried out between 24 and 72 h after surgery after full recovery. Imaging was performed under ketamine-Dexdomitor (100-0.5 mg/kg ip, 25% boosters). Atropine (0.03 mg/kg ip) was administered at the start of imaging and every 2 h hereafter. Eye lubricant was used throughout (Lubrifresh P.M. lubricant eye ointment).

Simultaneous recordings of the dorsal and lateral OB were made with two identical setups consisting of two Hamamatsu ORCA Flash 4.0 LT sCMOS cameras (Hamamatsu, Japan) at a frame rate of 30 Hz and with 4 × 4 binning to 512 × 512 pixels. Two high-power LED 470 nm (Thorlabs, Newark, NJ) were driven by a T-Cube LED Driver (LEDD1B; Thorlabs, Newark, NJ). The custom-made tandem-lens type (42) was used at a 2.7 magnification (FOV: 5 × 5 mm). Imaging lenses were prime Nikon F-mount (ccd lens: 135 mm f/3.5, used at f/8; object lens: 50 mm f/3.5, used at f/3.5). Custom code written in LabVIEW (National Instruments) controlled simultaneous image acquisition with both sCMOS cameras and timing controls for the light source and odor delivery. Sniffing and odor presentation data were acquired simultaneously through a National Instruments data acquisition device.

Each imaging session consisted of manually triggered trials with intertrial intervals of ≥2 min. Each trial consisted of 12 s of imaging where an odor was presented in one 3-s pulse with a custom-built multichannel auto-switching flow dilution olfactometer (43) with dedicated lines for each odor to avoid cross-contamination. Odorants were presented orthonasally to the animal at concentrations of either 0.1% or 1% of saturated vapor (% s.v.). Saturation was maintained by a flow (0.5 or 5 mL/min for 0.1% or 1% s.v., respectively) of filtered high-purity nitrogen (Airgas, NI ISP300, <0.1 ppm THC, H_2O and O_2 contaminants, 99.9999%) passing through passivated stainless steel spargers (IDEX health and science, A-243, 2-μm inlet filter) in PFA vials (Savillex 200-30-12) connected to the nose chamber (Figure 1A in Ref. 10) via an air-dilution manifold. Odors were diluted with clean air (Airgas, AI UZ300, ultra zero grade, <1 ppm THC, CO_2 and CO contaminants, batch analysis: 20.8% O_2, 0.023 ppm THC, 0.27 ppm moisture, 99.999%) at a flow rate of 499.5 or 495 mL/min for 0.1% or 1% s.v., respectively, for a constant combined air-nitrogen-odor flow rate of 500 mL/min into the nose chamber. The nose chamber consisted of a 1 × 0.5 × 1-in. (W × H × D) Teflon block with two 5-mm-inner diameter (ID) channels 10 mm from the front of the block. This allowed connection of a 1/8-in.-outer diameter (OD) Teflon tube for diluted odor flow into one side and a vacuum connection (4-mm ID, 8-mm OD Tygon) for outflow on the opposing side. Flow of odorants was continuous and was removed via the vacuum (2.5 L/min), which was switched off for odorant delivery. A central channel of 6-mm ID connected the orthogonal odor-vacuum stream to the frontally placed nares. The tip of the mouse's nose (including just the nares, OD 2 mm) was placed just inside the chamber, whereby there was ~2 mm of space surrounding the entire nose for unrestricted flow. Odorants (Sigma-Aldrich) used were heptanone, hexanal, amyl acetate (AA), carvone, methyl valerate (MV), and heptanol (stored under nitrogen in the dark). Mice were freely breathing, which was continuously measured by a piezoelectric strip positioned on the animal's thorax.

Initial Data Analysis

Custom code written in LabVIEW was used to extract the fluorescence traces from each trial. Frame subtraction was performed by selecting video frames just before and after odor presentation. This presented an image that highlighted regions that responded to odor stimulation. Multiple regions of interest (ROIs) that resembled glomeruli were manually selected per mouse. This process was repeated for all trials, and additional ROIs were selected to accumulate all glomeruli that responded in a particular mouse for all odors and all concentrations. This accumulated list of ROIs enabled direct comparison of the responsiveness of all glomeruli across odors. The ROIs were used to extract mean fluorescence intensity traces from time series images of all trials. All data are presented as means ± SE, except where indicated.

Data Overview

For each trial the optical imaging response traces (1 txt file for all ROIs per trial), ROI location [of the diagonally opposed corners of the rectangular area; no more than 50 per imaged OB area (lateral/dorsal) per animal; a txt file], and sniffing and odor presentation timing traces (a txt file) were analyzed in MATLAB (R2018a; The MathWorks, Natick, MA). The data set consisted of five animals each with up to 18 trials (5 or 6 odors × 2 or 3 trials) and up to 1,000 ROIs.

All data were referenced to the very stable OB imaging sampling times (virtually jitter-free 30.00 fps), to which odor and sniffing data were resampled and then shifted for proper alignment, followed by truncation. Alignment was verified by comparing an optically imaged LED driven in parallel by the odor-on vacuum valve with that of the odor valve txt file. The offset between the imaged data and odor/breathing data did not vary between trials.

First Odor Response

The start of inhalation with the piezo sensor (once band-pass filtered) was a sharp downward deflection after a relatively shallow downward slope, verified by coimaging of the thorax movement of a mouse. The timing thereof was determined by band-pass filtering (4th order, 1–10 Hz, zero phase shift) of the *z*-scored piezo voltage signal, followed by peak detection, from which the onset could reliably be determined with the sampling rate 30/s, or the interval between samples 33.3 ms. We identified the inhalation onset time for each trial that evoked the first dorsal OB response during presentation of odor ("odor on response"; odor on from 3.4 to 6.4 s) by finding the largest response within the series of fitted responses (see below) averaged across ROIs for the period 2.8–4.5 s. The subsequent five sniff responses were also included in the analyses.

Estimation of Firing Rate

For the information theoretic analyses, we assessed the first five odor sniff responses during two or three trials per odor

Table 1. *Information and percent correct from populations of mouse glomeruli measured from both the response magnitude and timing, from the magnitude only, and from the timing only*

Anim	D/LOB	nglom	nstim	Sparse	InfTot	InfRate	InfTime	PcTot	PcRate	PcTime	Chance	sigr	sigrmin
1	D	43	6	0.87	1.48	1.76	0.07	74.7	82.3	20.3	16.7	0.69	0.02
1	L	31	6	0.88	0.94	1.07	0.20	53.2	57.0	25.3	16.7	0.58	0.00
2	D	35	6	0.63	1.29	1.36	0.00	60.7	59.6	10.1	16.7	0.82	0.17
2	L	33	6	0.86	0.28	0.47	0.01	24.7	32.6	11.2	16.7	0.58	0.01
4	D	57	6	0.85	1.47	1.65	0.21	66.7	72.7	30.3	16.7	0.56	0.00
4	L	30	6	0.80	1.92	2.07	0.37	48.5	82.8	38.4	16.7	0.84	0.41
5	D	36	5	0.84	1.25	1.27	0.10	70.3	71.6	33.8	20.0	0.45	0.00
5	L	28	5	0.87	1.22	1.18	0.07	73.0	60.8	25.7	20.0	0.61	0.00
6	D	28	6	0.81	1.33	1.53	0.03	57.3	68.5	16.9	16.7	0.64	0.00
6	L	9	6	0.86	0.96	1.11	0.06	51.7	60.7	20.2	16.7	0.67	0.09

Information and percent correct from populations of mouse glomeruli measured from both the response magnitude (rate) and timing (InfTot), from the magnitude (InfRate) only, and from the timing only (InfTime). For this analysis, the mean response across all glomeruli for a single trial (i.e., sniff) to a given stimulus was set to the mean for that stimulus across all the trials for that stimulus. This removes sniff-to-sniff response variability that might be related to different sniff sizes for a given stimulus and any adaptation effect. This optimizes measurement of the information that is available from a population of glomeruli about which stimulus was presented in any 1 sniff. The analysis thus measures the information available from all glomeruli in any experiment on any 1 sniff. This removes trial-to-trial variability between sniffs. The information available from the time was for the time it took for the response to an odor to reach its half-maximal value. The mean Rate information across experiments was 1.35 ± 0.14 bits (mean ± SE), the mean information from the temporal measures was 0.11 ± 0.04 bits, and the mean total information was 1.21 ± 0.14 bits. Anim, mouse number; chance, percent correct by chance (= 100/nstim); D, dorsal olfactory bulb (DOB); InfRate, information (bits) from rates; InfTime, information (bits) from timing of response to half-maximum; InfTot, information total in bits from rate and time; L, lateral olfactory bulb (LOB); nglom, number of glomeruli; nstim, number of odor stimuli; PcRate, percent correct from rates; PcTime, percent correct from timing of response; PcTot, percent correct rate and time; sigr, signal correlation mean; sigrmin, signal correlation minimum; sparse, sparseness.

per mouse (n = 10–15 responses per odor per mouse) and we tested five or six odors per mouse (Table 1). Here we used a well-established approach to estimate glomerular firing rate based on the deconvolution of Ca^{2+} traces with the GCaMP6f response decay filter function (24). Traces were band-pass filtered (0.1–13 Hz; 4th-order Butterworth; MATLAB: filtfilt) and deconvolved (MATLAB: deconv) with an exponentially decaying filter with 0.142-s time constant using a zero-padded kernel. This time constant is the decay time constant of GCaMP6f in vivo in the mouse visual cortex (25). The resulting filtered traces, representing the estimated firing rate per glomerulus, were used for all analyses reported. We note that the absolute firing rate is not important for the calculation of stimulus information, as uniform scaling does not affect the relative response to the different stimuli and its variability that underlies the information measurement (19).

Fitting of Responses

To determine the peak response amplitudes (% ΔF/F) and temporal parameters (including time to reach a certain % of peak response) of the glomerular responses, we used a custom algorithm that fitted the optical signals from each ROI to a double-sigmoid function as described previously (44, 45). The analysis allowed robust and objective measurement of response timing. Briefly, the signal from each ROI, after each identified inhalation, was band-pass filtered [2nd-order Butterworth, 0.1–7 Hz] followed by 4th-order Daubechies wavelet decomposition (MATLAB function wden), soft thresholding of the coefficients at level 3, and then reconstruction. The response onset time was defined based on the time of peak in the product of the first and the second derivatives of the optical signal of each ROI. Starting at this time, each response was fitted (least-squares curve fitting) with a double-sigmoid function (a sigmoid rise followed by a sigmoid fall). The time of the peak of this response was defined as the peak in this fitted response function rather than the peak of the raw optical signal. The falling sigmoid was forced to asymptote to zero, thereby avoiding negative or sustained estimated firing rates (which could occur because of subsequent responses within the standardized 0.5-s period of each fitted trace). The double-sigmoidal responses were fit with low error (r = 0.86–0.94), and only a few responses (4.4%) could not be fitted and were not included in any of the analyses. One exception was *mouse 2*, whose dorsal (d)OB and lateral (l)OB responses could not be fitted for 11.0% and 7.1%, respectively. *Mouse 3* was not included in the analyses because of a low number (3) of stimuli. Supplemental Table S1 (all Supplemental Material is available at https://doi.org/10.6084/m9.figshare.21197914) provides further details. A total of 28,870 individual glomerular responses were included in this study,

For the information theoretic analyses described here, the mean response across all glomeruli for a single trial (i.e., sniff) to a given stimulus was set to the mean for that stimulus across all the trials for that stimulus. This removes sniff-to-sniff response variability that might be related to different sniff sizes for a given stimulus and any adaptation effect. This optimizes measurement of the information that is available from a population of glomeruli about which stimulus was presented in any one sniff. The analysis thus measures the information available from all glomeruli in any experiment on any one sniff. Supplemental Table S2 provides further details.

Data Sets for Information Analysis

We generated two data sets per mouse. One data set (for the dOB dOB_traces_dblsig and for lOB lOB_traces_dblsig) was generated to perform temporal frame-by-frame analyses (trials × ROI × odor sniff × frame; maximum sizes: 3 × 50 × 5 × 15), containing traces over 15 samples (0.5 s) of odor response based on their double-sigmoid fits. The second data set (for dOB dOB_trial_t10_ON, dOB_trial_t50_ON dOB_trial_t90_ON, dOB_trial_tpeak_ON; similar for lOB) was generated to test

information content in dynamics descriptors [time to reach 10% (t10), 50% (t50), and 90% (t90) of maximum response and peak (tpeak)] of their double-sigmoid fits (trials × ROI × odor sniff; maximum sizes: 3 × 50 × 5).

For a response parameter to carry information about which odor was presented, it must reliably be different across the stimuli. As a first pass we therefore performed a two-way ANOVA (MATLAB function anovan) of glomeruli responses, odors, and their interaction on each response parameter (t10, t50, t90, and Rate). Rate invariably showed extremely significant odor-glomeruli interactions, whereas t90 of lOB and dOB glomeruli was significant for *mice 2*, *4*, and *6*. It is hence unlikely for t90 in *mice 1* and *5* to carry information about odors. Supplemental Table S3 provides further details, and Supplemental Fig. S2 shows as an example the mean and SE of the t90 for *mouse 2*.

The Information Measurement Algorithm

The aim is to measure how much information is provided on average on a single trial, i.e., a single sniff, about which odor stimulus was presented, using measures of the responses of a population of glomeruli. The measures of the responses of each glomerulus might include the firing rates and one or more temporal measures such as the latency of the responses. In the present study, three temporal measures were used for each neuron, the time on each trial for the glomerulus to reach 10% (t10), 50% (t50), and 90% (t90) of its maximal response. We wish to measure the information from the rate alone, from the temporal measures alone (to compare their magnitude), and from both the rate and the temporal measure (to show whether there is additive information, which would indicate independence of the rate and temporal measures, with the alternative being redundancy). We note again that Shannon information theory (15) provides a principled approach to this type of question, because information measures are additive if they are independent, and the amount of information can be directly compared from different measures, including for example neuronal, fMRI, and behavioral measures (16–19). In the present application, the responses of a glomerulus are treated in the same way as the responses of a neuron, given that the neurons in a glomerulus have the same tuning to the stimuli and given that the response of a glomerulus as measured here reflects the firing rates of the neurons in the glomerulus (25).

The direct approach is to apply the Shannon mutual information measure (15, 46)

$$I(s,\ \mathbf{r}) = \sum_{s\in S}\sum_{\mathbf{r}} P(\mathrm{s},\mathbf{r}) \log_2 \frac{P(s,\mathbf{r})}{P(s)\,P(\mathbf{r})} \qquad (1)$$

where $P(s,\mathbf{r})$ is a probability table embodying a relationship between the variable s (here, the stimulus) and $\mathbf{r}$ (a vector that includes the response of each neuron and might be extended to include its firing rate and a temporal measure or measures such as latency).

However, because the probability table of the relation between the neuronal responses and the stimuli $P(s,\mathbf{r})$ is so large (given that there may be many stimuli and that the response space that has to include temporal information is very large), in practice it is difficult to obtain a sufficient number of trials for every stimulus to generate the probability table accurately, at least with data from mammals in which the experiment cannot usually be continued for many hours of recording from a whole population of cells. To circumvent this undersampling problem, Rolls et al. (40) developed a decoding procedure, in which an estimate (or guess) of which stimulus (called s') was shown on a given trial is made from a comparison of the neuronal responses on that trial with the responses made to the whole set of stimuli on other trials. One then obtains a conjoint probability table $P(s,s')$, and then the mutual information based on probability estimation (PE) decoding (I_p) between the estimated stimuli s' and the actual stimuli s that were shown can be measured:

$$\langle I_\mathrm{p}\rangle = \sum_{s\in S}\sum_{s'\in S} P(s,\ s') \log_2 \frac{P(s,s')}{P(s)\,P(s')} \qquad (2)$$

$$= \sum_{s\in S} P(s) \sum_{s'\in S} P(s'|s) \log_2 \frac{P(s'|s)}{P(s')} \qquad (3)$$

These measurements are in the low-dimensional space of the number of stimuli, and therefore the number of trials of data needed for each stimulus is of the order of the number of stimuli, which is feasible in experiments. The information values presented here are with this information analysis procedure in which the probabilities that it is each of the S stimuli are taken into account (i.e., probability estimation decoding). When providing the percent correct, this is based on the single stimulus that on a single trial has the highest probability, and therefore the percent correct does not follow exactly the information calculated using the probability for each stimulus on a trial (see further the Supplemental Material and Ref. 40).

To decode the probabilities that on a given trial each of the stimuli had been presented, a probability estimation leave-one-out cross-validation decoding procedure was used as described in detail in the Supplemental Material and illustrated in Supplemental Fig. S1 (see also Refs. 40 and 41). The decoding procedure allowed the information to be measured from the rates of each glomerulus in the population, from up to three temporal measures such as latency for each glomerulus in the population, or from both.

The selectivity of each glomerulus was measured by the sparseness measure a, which is widely used in quantitative analyses of the selectivity of neurons or neuronal populations, partly because it can also be used in analytic research on how sparseness influences memory storage in biologically plausible memory networks (18, 47–49). The single neuron sparseness, a^s, is

$$a^s = \left(\sum_{s=1}^{S} \frac{y_s}{S}\right)^2 \Big/ \left(\sum_{s=1}^{S} \frac{(y_s^2)}{S}\right) \qquad (4)$$

where y_s is the mean firing rate of the neuron to stimulus s in the set of S stimuli. A value of sparseness of $1/S$ indicates responsiveness to only 1 of the S stimuli, and a sparseness of 1.0 indicates no selectivity to the different stimuli.

RESULTS

The data from an experiment are illustrated in Fig. 1, which shows the responses of one of the presynaptic glomeruli to the six odor stimuli from the dorsal olfactory bulb in *mouse 1* as a function of time after the odor delivery. For the

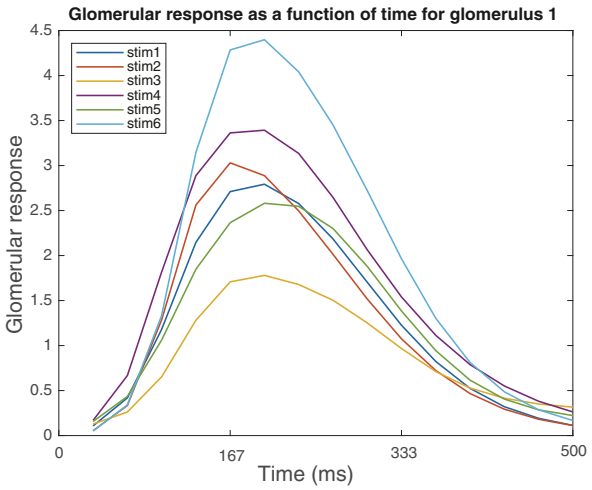

Figure 1. Poststimulus response of a single glomerulus to show a typical time course. This is for *mouse 1* dorsal olfactory bulb *glomerulus 1*. The estimated firing rates (deconvolved calcium response), labeled "glomerular response," are shown every 33.3 ms (the calcium signal imaging frame period) and are to each of the 6 odor stimuli. For the information theoretic measures described later, the Rate measure used was the sum of the activity between 0 and 500 ms. The sniff of the odor occurred at time *bin 1*. The odor stimuli in order are heptanone, hexanal, amyl acetate, carvone, methyl valerate, and heptanol.

information analyses, the magnitude of the response to 1% s.v. odorants was measured as the total activity over the first 15 bins (0.5 s) after inhalation onset, and the term "Rate" is used because the response is thought to reflect the firing rate of the neurons in a glomerulus (25). The temporal aspects of the response were measured by the times when the response to 1% s.v. odorants had reached 10%, 50%, and 90% of its maximum.

Glomeruli Have Broadly Tuned Response Profiles

The response profiles of typical glomeruli to the set of six stimuli are shown in Fig. 2. Ten glomeruli were selected at random from *experiment 1* in the dorsal olfactory bulb. It is clear that the glomeruli are not very selective for different odors. Indeed, we can see that the profiles of all these glomeruli are somewhat similar to the first four odor stimuli, and it is mainly for olfactory *stimuli 5* (methyl valerate) and *6* (heptanol) that the glomeruli have differences in their responses and could therefore provide evidence about which odor was presented. Figure 2*B* shows as an example that the correlations between the representations of the six olfactory stimuli by the population by 43 glomeruli in the dorsal olfactory bulb of *mouse 1* are mostly high, and the main stimulus that is different is *stimulus 6*, heptanol. This analysis shows that the response profiles by the population of glomeruli to the set of six odors are quite highly correlated with each other. That implies a poor representation of the set of stimuli, which was investigated as described next. Moreover, the different representation of *stimulus 6* by this set of glomeruli is evident in the Rate responses shown in Fig. 2*A*.

Similar results were found in all the experiments, with the correlations between the response profiles of each pair of glomeruli quite high in all experiments, as shown in Table 1 (Sigr). The mean value across experiments of this correlation of the response profiles of glomeruli or "signal correlation" for this set of six odor stimuli was 0.64. This shows quantitatively that the different glomeruli did not have on average very different tuning to the set of six stimuli, which implies poor encoding. At the same time, the minimum correlation between the response profiles of some pairs of glomeruli could be quite low (Table 1, Sigrmin with a mean value of $r = 0.07$), indicating that in most experiments some glomeruli did have different response profiles to this set of six odor stimuli. A quantitative measure of the selectivity of each glomerulus to the set of six odors is considered next.

A Very Nonsparse Distributed Representation of Odors as Shown by the Sparseness

The sparseness of the representation of the six stimuli is shown for each of the 330 glomeruli in Fig. 3. Across all 330 glomeruli on all five mice together, the mean of the sparseness was 0.83 ± 0.10 (mean ± SD) (see Fig. 3 and Table 1). This indicates quantitatively very broad tuning of each glomerulus to the set of six odor stimuli and a nonsparse distributed representation.

Information Is Encoded in the Magnitude of the Response (Rate) with Little Temporal Information from the Time of Arrival

The amounts of information that could be extracted from the responses of the population of glomeruli recorded in each experiment on any single trial (i.e., sniff) are shown in Fig. 4 and Table 1. This shows first that there is some information about which of the typically six odors was present from the magnitudes of the responses (rates) of the population of glomeruli recorded in each experiment. The mean information from the rates was 1.35 ± 0.14 bits (mean ± SE). For six odors, the amount of information needed to encode the six stimuli is 2.58 bits ($\log_2$ of the number of stimuli), so these sets of glomeruli imaged in each experiment were not sufficient to identify which of the six odors had been delivered from their responses on a single trial (sniff). That is reflected in the low percent correct for the identification of which odor was presented on a trial (mean = 65% correct for the 8 experiments with 6 stimuli for which chance = 16.7 correct as shown in Table 1).

Second, Fig. 4 and Table 1 show that a small amount of information was present in the temporal aspects of the responses of the glomeruli about which odor had been delivered on a trial (0.11 ± 0.04 bits), and, correspondingly, the percent correct from just the temporal aspects of the responses was just above the chance level (21.6% correct). As described in METHODS, the temporal response information was the time for the response to reach 10%, 50%, and 90% of its maximum response, for each glomerulus for each of the different odors . If any one or more of these provided reliable information for odor identification, that would be reflected in the amount of information that could be decoded from these temporal measures. The temporal measure provided in Table 1 is the information from the time to reach 50% of its maximum, and the information available from the time to reach 10% or 90% of the maximum response was similar.

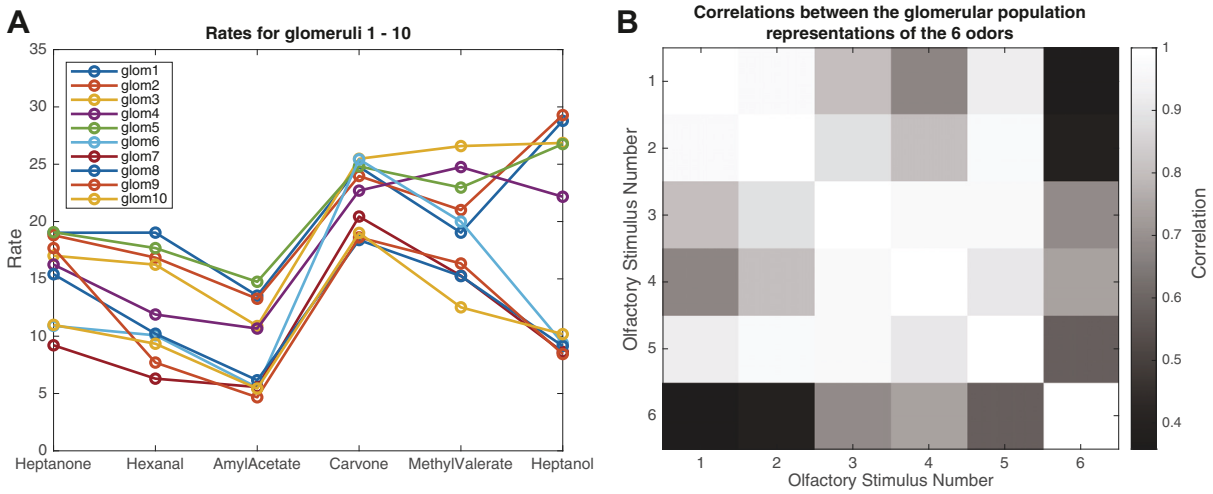

Figure 2. *A*: response (Rate) profiles of different glomeruli to the set of odors. The examples shown are typical of the entire recorded population and are the first 10 glomeruli in the set of 43 glomeruli imaged in the dorsal olfactory bulb of *mouse 1*. The Rates were those accumulated over time *bins 1–15* (0–500 ms), as by this time the information available had reached its peak value. *B*: the correlations between the representations by the population by 43 glomeruli of the 6 olfactory stimuli in the dorsal olfactory bulb of *mouse 1*. This shows that this population of 43 glomeruli separated *odor 6* (heptanol) from the other odors, in that the correlation of the responses to *odor 6* with the responses to the other odors was relatively low.

Third, Fig. 4 and Table 1 show that the total information available when taking into account both the firing rate and the temporal measure was 1.21 ± 0.14 bits (and 54.7% correct), no better than the information available from the rate alone. This was confirmed by a paired *t* test for the total information versus the rate information available in all 10 experiments ($t = -4.5$, df = 9, $P < 0.002$). (In fact, the total information was thus significantly lower than the information from the rate alone, with the reason for the small decrease of the total information that the latency information introduced noise into the decoding performed by the information measurement algorithm). The implication is that any information present in the temporal aspects of the neuronal response is redundant with respect to the firing rate. The concept of redundancy is described elsewhere (18, 19), but for the present purposes the point is that the information from the latency is not orthogonal to, i.e., is correlated with, the information from the firing rates of the glomeruli. The implication is that a rate code is sufficient to account for the encoding of information about odors by the glomeruli in the olfactory bulb.

The Information Becomes Available from the Glomeruli within 67 ms and Saturates by 100 ms after Odor Onset

Figure 5 shows how the information becomes available as a function of time for a typical experiment. The information is measured from the sum of the (GCamP6f decay time deconvolved) responses accumulated by the end of each time bin. By *bin 3*, representing the time period 0–100 ms after sniff onset, the maximal information had been reached.

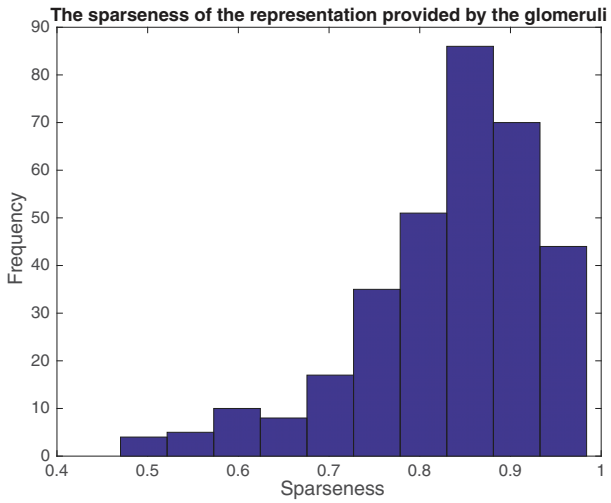

Figure 3. Frequency histogram showing the sparseness of the representations of the 6 odors provided by the 330 individual glomeruli to the set of 6 odors in the dorsal and lateral olfactory bulb in 10 experiments. The mean sparseness was 0.83, and the median sparseness was 0.85. A value of sparseness of 0.17 indicates responsiveness to only 1 of the 6 odors, and a response of 1.0 indicates no selectivity to the different odors.

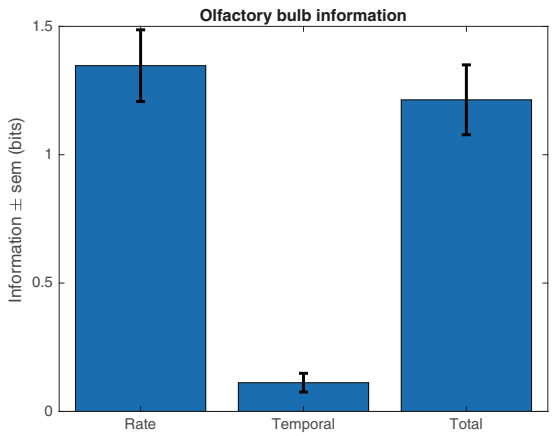

Figure 4. Information about which odor was presented from populations of typically 28–57 glomeruli in the olfactory bulb provided by the magnitude of the responses (Rate), the time course of the responses (Temporal), and the total from both the magnitudes and the time courses (Total). The values are averaged across all 10 experiments. The means and SE are shown.

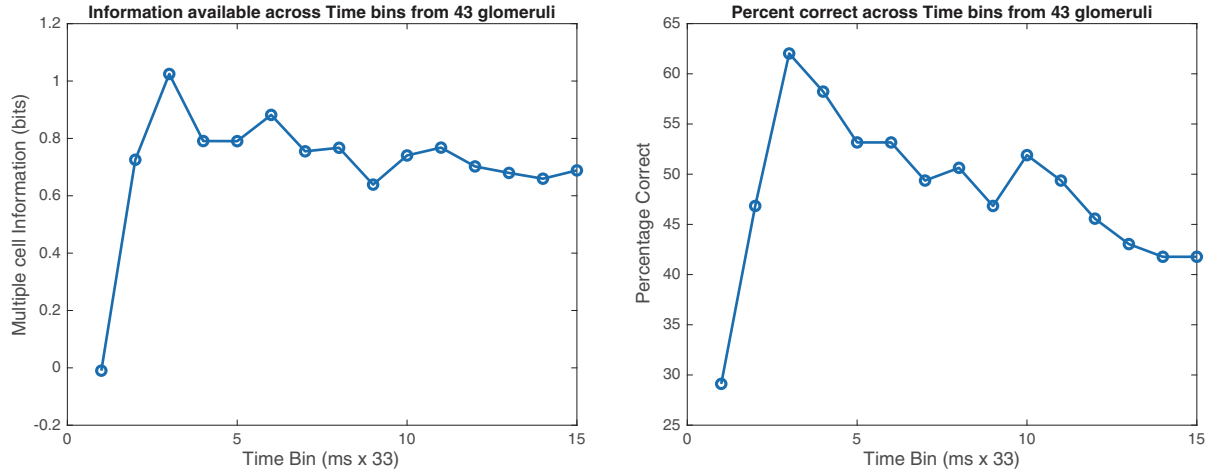

Figure 5. Information as a function of time after the onset of the odor. The information is measured from the sum of the responses accumulated by the end of each time bin. This is the information from 43 glomeruli about which of the 6 odors had been presented on a trial, from the dorsal olfactory bulb of *mouse 1*. The percent correct is shown on the *right*. By *bin 3*, representing the time period 0–100 ms after sniff onset, the maximal information had been reached. Some information was present by time *bin 2*, the time period 0–67 ms after sniff onset.

Some information was present by time *bin 2*, the time period 0–67 ms after sniff onset. An interesting implication of these findings is that although the activity of the glomeruli does continue for some time and then decreases after its peak (Fig. 1), all the information that can be extracted from the rates (and temporal information) is available by 100 ms after sniff onset. The small decrease in the information and the percent correct after the initial peak is likely to reflect variability in the later parts of the glomerular response.

The Information Increases for the First Few Glomeruli in a Set but Then Saturates

Figure 6 shows how the information about the six odors increased as more glomeruli were included in the analysis. The data are from the dorsal olfactory bulb of *mouse 1*, which are representative of all the experiments, and are the total information from the rate. The average amount of information from any one glomerulus was ~0.26 bits, from any two was ~0.42 bits, and from any three was ~0.62 bits. The increase of information as more glomeruli are used for the decoding rises steeply at first, indicating that the first few glomeruli provide somewhat independent information about which stimulus was presented. But after that, as more glomeruli were included in the analysis, the amount of information increased only slowly to a value of 1.76 bits (and 82% correct), far below the ceiling of 2.58 bits needed to decode which of the six odors had been presented. [The concept of an information ceiling is described elsewhere (40).] These findings are also reflected in the percent correct for the identification of which odor was presented on a trial (Fig. 6).

The implication is that there are considerable correlations between the encoding provided by different glomeruli, with the response profiles of the glomeruli to at least this set of stimuli showing considerable correlations (Table 1). These correlations are associated with considerable redundancy as the number of glomeruli in the population increases.

The overall implication is that glomeruli (at least these) are so broadly tuned to the stimuli (at least these stimuli) that there is much redundancy in their encoding, and a large number of glomeruli is needed to identify a set of odors.

The Information Encoded by Hundreds of Glomeruli

The correlation matrices between the stimuli illustrated in Fig. 2*B* were different for the different experiments shown in Table 1. This suggested that the sets of glomeruli in the different experiments were coding for different sets of stimuli. This in turn suggested that the representations of the stimuli might be less correlated if all the experiments with all the glomeruli were considered together. In information theory terms, if all the glomeruli could be combined in the readout of information, then the wider range of response profiles to the set of stimuli should increase the amount of information that could be represented.

It was possible to test this hypothesis by combining all the glomeruli that had been tested with six stimuli (hence excluding *mouse 5*). This produced 266 glomeruli for analysis (for both the dorsal and lateral olfactory bulb, from *mice 1*, *2*, *4*, and *6* as shown in Table 1). [With nonsimultaneously recorded neurons in this analysis, the information may be a little lower than with simultaneous recordings, because of trial-to-trial variation effects (40). Also, we note that by chance several of the glomeruli in the different experiments may have expressed the same olfactory receptor gene.] It is shown in Fig. 7 that now the information about the six stimuli from the rates reaches 2.58 bits, and the percent correct is 100%.

This is an interesting result, for with a number of glomeruli that is close to one-quarter of the number of olfactory receptor genes, the information does reach the amount of 2.58 bits needed to encode the six odors.

There Is Redundancy of Information in the Dorsal and Lateral Parts of the Olfactory Bulb

We tested whether the representation of information in glomeruli in the dorsal and lateral parts of the olfactory bulb was additive and therefore independent. It was found that there was no greater additivity of information across these

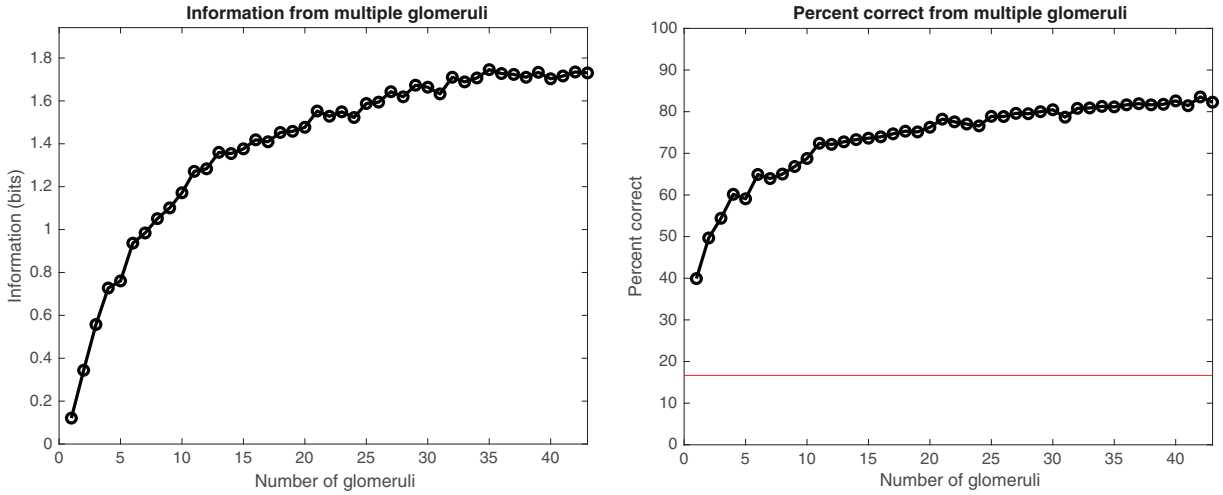

Figure 6. Information and percent correct as a function of the number of glomeruli. The analysis was for the information from the magnitude of the response (Rate). There were 6 olfactory stimuli, so the chance percent correct was 16.7% (red line) and the amount of information required to identify which odor was presented on a single trial (sniff) was 2.58 bits. The data are from the dorsal olfactory bulb of *mouse 1*.

two parts of the olfactory bulb than within either part. For example, for *mouse 1*, if the 74 glomeruli from the dorsal and lateral olfactory bulbs were combined, the information from the rate about the six odors was 1.67 bits with 75.9% correct, which is not above the information and percent correct for either olfactory bulb alone shown in Table 1. In fact, the values are between the values for each olfactory bulb separately, implying that in this case one bulb adds noise to the information otherwise available from the other olfactory bulb. Furthermore, if the performance was measured from a sample of 43 glomeruli selected at random from the lateral and dorsal olfactory bulb, then the information was 1.56 bits with 74.7% correct, which again is between the values from Table 1 if the glomeruli are from one of the bulbs alone. Consistent findings were produced for the other experiments. (For *mouse 2* for 68 glomeruli the rate information was 1.29 bits; for *mouse 4* for 87 glomeruli 2.02 bits; for *mouse 5* for 64 glomeruli 1.58 bits; and for *mouse 6* for 37 glomeruli 1.54 bits.) The implication is that the information about stimuli that is represented in the dorsal and lateral parts of the olfactory bulb is not orthogonal but is similar, at least as tested with the set of six odors used in this investigation.

DISCUSSION

The research described here makes a number of key points about the encoding of information by presynaptic inputs to olfactory bulb glomeruli. We note that given that each glomerulus receives input from one type of ORN, the output of each glomerulus is likely to reflect its inputs described here, although, e.g., lateral inhibition between glomeruli might decorrelate the glomerular outputs (50–54). First, the tuning of the glomeruli to a set of odors is remarkably broad, i.e., unselective for particular odors (Figs. 1 and 2), and this is

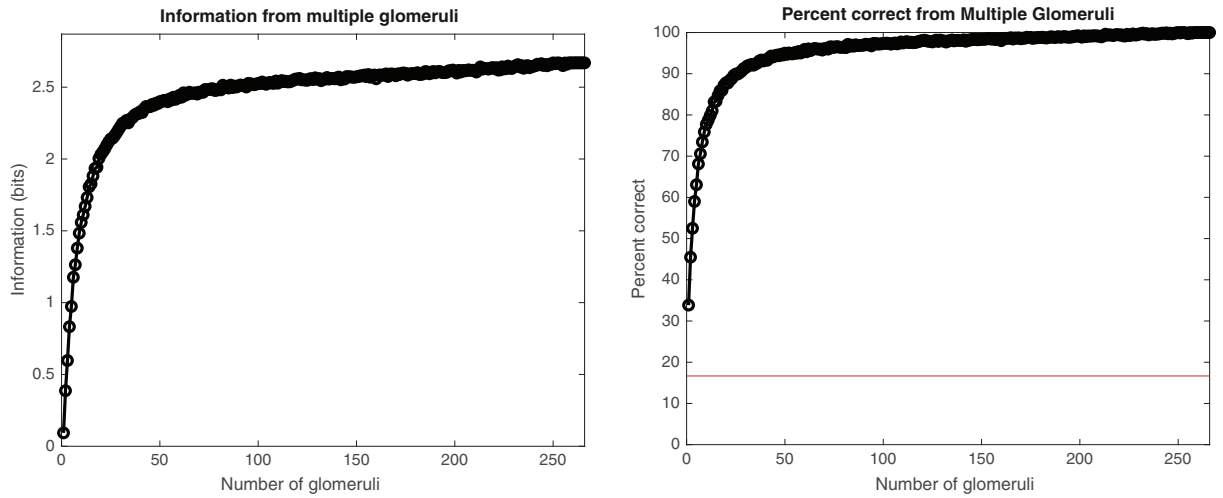

Figure 7. Information and percent correct as a function of the number of glomeruli up to 266 glomeruli. The analysis was for the rate measure. There were 6 olfactory stimuli for these 4 mice, so the chance percent correct was 16.7% (red line) and the amount of information required to identify which odor was presented on a single trial (sniff) was 2.58 bits. The data are from the dorsal and lateral olfactory bulbs of animals presented with 6 odorants (*mice 1*, *2*, *4*, and *6*). The 266 glomeruli provided perfect encoding of the 6 odors.

measured by a very nonsparse representation (Fig. 3). There are thus quite high correlations between the response profiles of different glomeruli to the set of stimuli [Sigr in Table 1, known as "signal correlations" (17, 19)]. Second, both of these factors contribute to the rather low information that is available from the responses of even populations of tens of glomeruli (Fig. 4). As shown in Table 1, the information from the responses of even tens of glomeruli had a mean of 1.35 bits, whereas 2.58 bits of information are required to encode this set of six olfactory stimuli. It was only when the information was read from 266 glomeruli that the information required to decode the identity of each of the six odors reached the required 2.58 bits and the performance for identifying the most different odor became 100% correct (Fig. 7). Third, although there is considerable interest in the possibility of temporal encoding of stimulus including odor identity (27–29), it was shown here with information theoretic methods that the amount of information in the temporal aspects of the glomerular responses was low and, importantly, was redundant with respect to the information available from the rates (Fig. 4 and Table 1). Fourth, in line with a large role for earliest-responding neurons (35), it was found that much of the information available to discriminate between the six odors became available rapidly, by 100 ms (Fig. 5), well before the peak of the response occurred (Fig. 1). Fifth, it was shown that reasonable amounts of information were available from the lateral as well as from the dorsal olfactory bulb (Table 1) but that the information from the lateral and dorsal bulbs was not orthogonal (i.e., was not different about the set of odors). Some of the implications of these advances are now considered.

The finding that there is so little information from even tens of glomeruli about which of six odors was presented in a trial (Fig. 4 and Table 1) has profound biological implications. An implication is that very large numbers of glomeruli may be needed because the genes are able so poorly to specify very odor-selective olfactory receptors in mammals [which of course defines the tuning of glomeruli, in that each gene-defined olfactory receptor type connects to a different glomerulus (1–3)]. The lack of selectivity of the glomeruli is shown also by the high signal correlations between the response profiles of the neurons (Sigr in Table 1). The relatively low minimal value for the signal correlation (Sigrmin in Table 1) indicates that the glomeruli could separate at least one pair of the odors well, but the relatively high value of Sigr is evidence that not all of the six odors were separately represented well, for the profiles are rather highly correlated. Further evidence for the poor selectivity of the glomeruli is that the mean sparseness of the representation of the six odors for each of the glomeruli was 0.83, where the scale is from 1/6 indicating responsiveness to one odor to 1 representing equal responses to all odors (Fig. 3). It is proposed that the evolutionary reason why so much of the mammalian genome (1,000 genes, 1/30th of the total number) is devoted to building 1,000 different olfactory receptor types is not only that the behaviorally relevant odor space is large but also because each receptor type discriminates rather poorly between a set of odors, so that enormous numbers (1,000) of genes must be devoted to specifying all of the 1,000 receptor types.

The analysis shown in Fig. 7 with 266 glomeruli supports these views, in that with a number of glomeruli that is close to one-quarter of the number of olfactory receptor genes the information reaches the 2.58 bits needed to encode the identity of each of the six odors in a single sniff. The implication is that as more glomeruli are added to the sample, their somewhat different response profiles gradually allow which odor was presented to be decoded.

There is a real difference here from the taste system. In the taste system, which encodes a much smaller stimulus space, there are five taste qualities, sweet, sour, bitter, salty, and umami, with a relatively small number of taste receptors (55). The cortical neurons that represent the signals transduced for the five taste types encode a great deal of information about which taste is presented in a single trial (56). It is suggested that because of the much easier task of specifying taste receptors, with the high concentration of the stimuli, genes find it much easier to specify taste receptors than genes can define receptors for odor molecules that are typically present in much lower concentrations.

Odors were carefully selected *1*) that activate the dorsal and lateral OB based on 2-deoxyglucose (2-DEOG) work (57–59), *2*) that have been widely used in the optical imaging literature (for comparisons), and that are *3*) detectable and likely discriminable by rodents (e.g., Refs. 60–62) and *4*) relatively small in number to allow the large number of repetitions necessary to reduce bias of the information theoretic estimates. We furthermore used monomolecular odorants to avoid mixture interactions (cross-habituation, inhibition), and tested odor quality information at 1% s.v. Although this comprehensive odorant set yielded a large data set that was highly suited for our optical information theoretic approach, these selection criteria naturally also limit the span of the odor space of the odorants, but it is not possible to test with very large numbers of the possible enormous range of odorants.

Low signal-to-noise ratio could also reduce odor specificity; however, the ANOVAs for each mouse and OB area for the evoked rates in Supplemental Table S3 show that, invariably, evoked estimated activity is very highly significantly ($P < 0.001$) dependent on odor as well as glomeruli and their interaction. This strongly suggests that trial-to-trial or sniff-to-sniff variability plays a minor role in the information that can be extracted about odor identity from the responses of the glomeruli and that instead a key factor in the low amount of information available is the broad tuning of the glomeruli to the odors for which an example is provided in Fig. 1.

Furthermore, in our original paper (10) we show the average *z* scores of glomerular response amplitudes, relative to preodor breathing response amplitudes (cf. Figure 2D in Ref. 10). This demonstrates that responses to odors typically reach several times (>3) the preodor variation. Hence the signal-to-noise ratio is high and does not explain the lack of selectivity.

As outlined in INTRODUCTION, the sparseness of ORN tuning has been shown to be strongly concentration dependent. Thus, the relevance of our present results, based on relatively high odor concentrations and relatively continuous odor presence (high intermittency), on population-wide rate-based odor information may well apply especially to conditions where the observer is close to the odor source, e.g., during food exploration and ingestion. Indeed, it has been reported that presenting natural stimuli close to the nose evokes dense glomerular activity in

mice, equivalent to its main monomolecular analog at equi-intense concentration (63).

Recent research has shown that 1% s.v. was typically roughly centered of the steep concentration-response curve of mouse ORNs across a 2-log odor concentration range (Figures 2D, 3D, and 4D in Ref. 64). This argues in favor of physiological relevance of the concentration used in the present investigation.

It is interesting that in the olfactory bulb the encoding of information is by the rate of neurons (reflected in the signal recorded here), with no additional information provided by the time course of the response and in particular the latency of the glomerular responses measured here. (The time course was included in the information analysis in that it used the times for the responses of each glomerulus to respond to each odor with 10%, 50% and 90% of the maximum response to each odor.) This helps to establish this principle as a general principle of information encoding in the brain, for the same is found in the primate inferior temporal visual cortex, in which there is a small amount of information in the latency of neuronal responses, but it is redundant with respect to the information available from the firing rates of the neurons (17–19, 41, 65–68).

We believe that the sampling rate of 33.3 ms was sufficiently fast to enable possible differences in response latency to different odors to be measured based on the following. First, there are approximately six measures of the response before the response reaches its peak (see, e.g., Fig. 1). These six time points should be sufficient to decode temporal information. It is possible, but unlikely, that at some time between the measures spaced at 33-ms intervals there was some difference in the response that was not evident at the start or end of any 33-ms period, but that is rather unlikely. Third, the fact that the rate information saturates at ~100 ms does not entail at all that there is no information from the temporal aspects of the response over the first six time bins, for the temporal information was measured in the "temporal" analysis without taking into account at all the Rate information. Fourth, if any temporal information was available, it would be likely to be evident early on in the response, but as described in METHODS the temporal information measure did take into account any information that might be available early on at the time that the response had reached 10% of its peak height, but there was still little information available from the time of arrival. We further note that the time course of glomerular responses across the olfactory bulb spans ~200 ms and differences in t90 occur up to ~100 ms (26, 45), which are discriminable down to 15 ms (69). Higher sampling rates may hence refine the accuracy of capturing the timing of responses, but the majority of temporal variance is already captured at 30 Hz. Increased sampling rates are hence not expected to change the major difference in the information from the latency of the glomerular responses to different odors.

A striking property of the glomerular responses found here and in the optical imaging OB literature generally (e.g., Refs. 11, 45) is that they are relatively transient and coherent with the sniff cycle and last for a much shorter time than the stimulus delivery time of 3 s (Fig. 1). Figure 1 shows that the glomerular response associated with each sniff has a peak at ~200 ms and lasts for ~500 ms. This transient nature of the response is not found in neurons with olfactory responses in the macaque orbitofrontal cortex (a secondary cortical olfactory area) (56, 70–72) and may not be very evident in human subjective experience, in which the subjective intensity of an odor does not wax and wane to the same extent as OB activity does with every sniff. It is likely that the recurrent collateral connections in the pyriform cortex and orbitofrontal cortex may perform this temporal smoothing by acting as attractor networks (19).

It is also of interest that the information becomes available relatively fast, within 100 ms of the sniff onset (Fig. 5), and before the peak response (Fig. 1). This is in line with odor-guided behavioral decisions occurring during the time course of bulbar response development (e.g., Ref. 44) and the notion of primacy coding (39). An advantage of fast processing at each stage of information processing in neural systems is that when several stages follow each other in a hierarchy the time to the final output from the hierarchy is made available sufficiently fast to enable a fast behavioral response to be made to what could be a life-threatening stimulus. For comparison, there is clear evidence that the time for each stage of the primate cortex (e.g., V1, V2, V4, inferior temporal cortex for the visual system) is ~15 ms per cortical stage, resulting in information about the identity of a visual stimulus to be available in the macaque inferior temporal visual cortex within 100 ms of visual stimulus onset (18, 19, 65, 73–75).

As the olfactory processing continues up the hierarchy of stages through the pyriform cortex to the orbitofrontal cortex, the representations are expected to become more sparse but still distributed, and less correlated, as this increases the storage capacity of associative neuronal networks in the brain (18, 19, 48, 49, 56). This does occur for primates (56, 70, 71, 76), and may also occur in rodents (77, 78).

The analyses performed here show that the tuning of the mouse glomeruli is rather broad to the set of odors and that rather low amounts of information can be read out from the olfactory bulb about which odor was presented on a single trial. How the information is encoded is important for how easily information can be read out from a population of neurons. For example, it is very difficult to read out much information about which face is being viewed from retinal ganglion cell responses especially when the faces of individuals occur with different transforms of position, size, etc. on the retina, but this can be performed easily by recording from a few neurons in the cortex in the macaque inferior temporal visual cortex (IT) (17, 19, 65, 73, 74, 79). The reason for this is that the information has been recoded into an invariant representation in the inferior temporal visual cortex that is well suited to decoding which face has been shown independently of transforms. The same issues may be present in the olfactory system. It may be easier to read the information out from later stages in olfactory processing about what odor was presented because of the great deal of processing performed in cortical regions. Indeed, from only 24 neurons in the macaque orbitofrontal cortex, it is possible to read out 1.05 bits of information about which odor was presented (a mean of 0.044 bits per neuron) and to identify an odor at 65% correct (56). For the glomeruli investigated here, the information was 1.35 bits from populations of 28–57 glomeruli, or very approximately 0.04 bits per glomerulus. Although the amount of information per single orbitofrontal cortex neuron or whole mouse

glomerulus is similar, a closer comparison would require the same odors and species to be compared. But the comparison is quite revealing, for the information in the orbitofrontal cortex rises linearly with at least this number of neurons (56), and there are tens of thousands of olfactory neurons in macaque cortical regions. So at least in the macaque cortex the evidence about what odor was presented on a single trial is encoded in a form that makes it likely that which odor from a large number was presented could be identified. The encoding in the mouse olfactory bulb described here may be less suitable for an odor identification computation but instead what is possible for the olfactory receptors/glomeruli to encode because of their broad tuning to odors.

A potential limitation of any analysis of encoding is that what is found is likely to depend on the stimulus set. In the experiments described here, six odors were used that are probably easily discriminable by mice. The considerable set of glomeruli from which recordings were made in the 10 experiments described here did not discriminate between this set of odors very well, but some mitral and tufted cells (the projection neurons) in glomeruli can be quite selectively tuned to odors (3). It will be useful to extend the investigations described here with different sets of odors. Another potential limitation is that the responses of the glomeruli measured under anesthesia may show more adaptation (which we attempted to adjust for), and may be more variable, than if the measurements were made in an awake animal performing an olfactory discrimination task in which the animal would ensure efficient sample and processing of the olfactory stimuli.

Conclusions

To our knowledge, this is the first information theoretic analysis of how information about odor stimuli is represented across a population of glomeruli in the olfactory bulb. It was found that the tuning of the presynaptic glomeruli to a set of six odors was distributed and nonsparse (the mean sparseness was 0.83), with relatively high "signal" correlations between the responses of the neurons to the different odors (mean = 0.64). Consistent with this, the information available from any one glomerulus was typically low (~0.2 bits), and the glomeruli had relatively nonindependent responses, so that the information increased more and more gradually to a mean of 1.35 bits across a population of ~33 glomeruli, whereas 2.58 bits were needed to encode the six stimuli. Only when the information was decoded from 266 glomeruli across the different experiments did the information reach 2.58 bits and 100% correct. It was found that most of the information was available from the magnitude of the responses, and not from the latency measures, and that the latency measures were redundant with respect to the rate measure. The information from a population became available quite rapidly, within 100 ms of sniff onset, whereas the peak of the glomerular response was at 200 ms. It was also found that the information from the lateral olfactory bulb was not additive with that of the dorsal olfactory bulb.

CODE AVAILABILITY

Programs written in MATLAB that perform the multiple cell information analyses described here are available in connection with *Cerebral Cortex: Principles of Operation* (18) and *Brain Computations: What and How* (19) at https://www.oxcns.org/NeuronalNetworkSimulationSoftware.html.

DATA AVAILABILITY

Data will be made available upon reasonable request.

SUPPLEMENTAL MATERIAL

Supplemental Material: https://doi.org/10.6084/m9.figshare.21197914.

GRANTS

This work was supported by NIH/NIDCD Grant R01DC014723 and National Science Foundation (NSF) Grant BRAIN IOS-1555880 to J.V.V. as well as NIH NS099714 and NS103517 to V.A.P. and Defense Advanced Research Projects Agency (DARPA) N66001-17-C-4012 to V.A.P. This project is supported by the NSF/CIHR/DFG/FRQ/UKRI-MRC Next Generation Networks for Neuroscience Program (Award No. 2014217) to J.V.V.

DISCLOSURES

No conflicts of interest, financial or otherwise, are declared by the authors.

AUTHOR CONTRIBUTIONS

J.V.V., V.A.P., and E.T.R. conceived and designed research; K.L.B. performed experiments; J.V.V., K.L.B., V.A.P., and E.T.R. analyzed data; J.V.V., V.A.P., and E.T.R. interpreted results of experiments; J.V.V., V.A.P., and E.T.R. prepared figures; J.V.V., V.A.P., and E.T.R. drafted manuscript; J.V.V., K.L.B., G.V., V.A.P., and E.T.R. edited and revised manuscript; J.V.V., K.L.B., G.V., V.A.P., and E.T.R. approved final version of manuscript.

REFERENCES

1. **Zapiec B**, **Mombaerts P.** Multiplex assessment of the positions of odorant receptor-specific glomeruli in the mouse olfactory bulb by serial two-photon tomography. *Proc Natl Acad Sci USA* 112: E5873–E5882, 2015. doi:10.1073/pnas.1512135112.
2. **Mombaerts P.** Axonal wiring in the mouse olfactory system. *Annu Rev Cell Dev Biol* 22: 713–737, 2006. doi:10.1146/annurev.cellbio.21.012804.093915.
3. **Mori K**, **Nagao H**, **Yoshihara Y.** The olfactory bulb: coding and processing of odor molecule information. *Science* 286: 711–715, 1999. doi:10.1126/science.286.5440.711.
4. **Mori K**, **Sakano H.** How is the olfactory map formed and interpreted in the mammalian brain? *Annu Rev Neurosci* 34: 467–499, 2011. doi:10.1146/annurev-neuro-112210-112917.
5. **Mori K**, **Mataga N**, **Imamura K.** Differential specificities of single mitral cells in rabbit olfactory bulb for a homologous series of fatty acid odor molecules. *J Neurophysiol* 67: 786–789, 1992. doi:10.1152/jn.1992.67.3.786.
6. **Imamura K**, **Mataga N**, **Mori K.** Coding of odor molecules by mitral/tufted cells in rabbit olfactory bulb. I. Aliphatic compounds. *J Neurophysiol* 68: 1986–2002, 1992. doi:10.1152/jn.1992.68.6.1986.
7. **Zhu KW**, **Burton SD**, **Nagai MH**, **Silverman JD**, **de March CA**, **Wachowiak M**, **Matsunami H.** Decoding the olfactory map through targeted transcriptomics links murine olfactory receptors to glomeruli. *Nat Commun* 13: 5137, 2022. doi:10.1038/s41467-022-32267-3.
8. **Pfister P**, **Smith BC**, **Evans BJ**, **Brann JH**, **Trimmer C**, **Sheikh M**, **Arroyave R**, **Reddy G**, **Jeong HY**, **Raps DA**, **Peterlin Z**, **Vergassola M**, **Rogers ME.** Odorant receptor inhibition is fundamental to odor encoding. *Curr Biol* 30: 2574–2587.e6, 2020. doi:10.1016/j.cub.2020.04.086.

9. **Gautam SH**, **Verhagen JV.** Retronasal odor representations in the dorsal olfactory bulb of rats. *J Neurosci* 32: 7949–7959, 2012. doi:10.1523/JNEUROSCI.1413-12.2012.
10. **Baker KL**, **Vasan G**, **Gumaste A**, **Pieribone VA**, **Verhagen JV.** Spatiotemporal dynamics of odor responses in the lateral and dorsal olfactory bulb. *PLoS Biol* 17: e3000409, 2019. doi:10.1371/journal.pbio.3000409.
11. **Wachowiak M**, **Cohen LB.** Representation of odorants by receptor neuron input to the mouse olfactory bulb. *Neuron* 32: 723–735, 2001. doi:10.1016/S0896-6273(01)00506-2.
12. **Gautam SH**, **Short SM**, **Verhagen JV.** Retronasal odor concentration coding in glomeruli of the rat olfactory bulb. *Front Integr Neurosci* 8: 81, 2014. doi:10.3389/fnint.2014.00081.
13. **Braubach O**, **Tombaz T**, **Geiller T**, **Homma R**, **Bozza T**, **Cohen LB**, **Choi Y.** Sparsened neuronal activity in an optogenetically activated olfactory glomerulus. *Sci Rep* 8: 14955, 2018. doi:10.1038/s41598-018-33021-w.
14. **Platisa J**, **Zeng H**, **Madisen L**, **Cohen LB**, **Pieribone VA**, **Storace DA.** Voltage imaging in the olfactory bulb using transgenic mouse lines expressing the genetically encoded voltage indicator ArcLight. *Sci Rep* 12: 1875, 2022. doi:10.1038/s41598-021-04482-3.
15. **Shannon CE.** A mathematical theory of communication. *AT&T Bell Lab Tech J* 27: 379–423, 1948. doi:10.1002/j.1538-7305.1948.tb01338.x.
16. **Rolls ET**, **Grabenhorst F**, **Franco L.** Prediction of subjective affective state from brain activations. *J Neurophysiol* 101: 1294–1308, 2009. doi:10.1152/jn.91049.2008.
17. **Rolls ET**, **Treves A.** The neuronal encoding of information in the brain. *Prog Neurobiol* 95: 448–490, 2011. doi:10.1016/j.pneurobio.2011.08.002.
18. **Rolls ET.** *Cerebral Cortex: Principles of Operation*. Oxford, UK: Oxford University Press, 2016.
19. **Rolls ET.** *Brain Computations: What and How*. Oxford, UK: Oxford University Press, 2021.
20. **Rolls ET.** *Brain Computations and Connectivity*. Oxford, UK: Oxford University Press, 2023.
21. **Johnson BA**, **Leon M.** Chemotopic odorant coding in a mammalian olfactory system. *J Comp Neurol* 503: 1–34, 2007. doi:10.1002/cne.21396.
22. **Johnson BA**, **Ong J**, **Leon M.** Glomerular activity patterns evoked by natural odor objects in the rat olfactory bulb are related to patterns evoked by major odorant components. *J Comp Neurol* 518: 1542–1555, 2010. doi:10.1002/cne.22289.
23. **Johnson BA**, **Xu Z**, **Ali SS**, **Leon M.** Spatial representations of odorants in olfactory bulbs of rats and mice: similarities and differences in chemotopic organization. *J Comp Neurol* 514: 658–673, 2009. doi:10.1002/cne.22046.
24. **Yaksi E**, **Friedrich RW.** Reconstruction of firing rate changes across neuronal populations by temporally deconvolved Ca^{2+} imaging. *Nat Methods* 3: 377–383, 2006. doi:10.1038/nmeth874.
25. **Chen TW**, **Wardill TJ**, **Sun Y**, **Pulver SR**, **Renninger SL**, **Baohan A**, **Schreiter ER**, **Kerr RA**, **Orger MB**, **Jayaraman V**, **Looger LL**, **Svoboda K**, **Kim DS.** Ultrasensitive fluorescent proteins for imaging neuronal activity. *Nature* 499: 295–300, 2013. doi:10.1038/nature12354.
26. **Spors H**, **Wachowiak M**, **Cohen LB**, **Friedrich RW.** Temporal dynamics and latency patterns of receptor neuron input to the olfactory bulb. *J Neurosci* 26: 1247–1259, 2006. doi:10.1523/JNEUROSCI.3100-05.2006.
27. **Li A**, **Gire DH**, **Bozza T**, **Restrepo D.** Precise detection of direct glomerular input duration by the olfactory bulb. *J Neurosci* 34: 16058–16064, 2014. doi:10.1523/JNEUROSCI.3382-14.2014.
28. **Smear M**, **Shusterman R**, **O'Connor R**, **Bozza T**, **Rinberg D.** Perception of sniff phase in mouse olfaction. *Nature* 479: 397–400, 2011. doi:10.1038/nature10521.
29. **Rebello MR**, **McTavish TS**, **Willhite DC**, **Short SM**, **Shepherd GM**, **Verhagen JV.** Perception of odors linked to precise timing in the olfactory system. *PLoS Biol* 12: e1002021, 2014. doi:10.1371/journal.pbio.1002021.
30. **Connor EG**, **McHugh MK**, **Crimaldi JP.** Quantification of airborne odor plumes using planar laser-induced fluorescence. *Exp Fluids* 59: 137, 2018. doi:10.1007/s00348-018-2591-3.
31. **Lewis SM**, **Xu L**, **Rigolli N**, **Tariq MF**, **Suarez LM**, **Stern M**, **Seminara A**, **Gire DH.** Plume dynamics structure the spatiotemporal activity of mitral/tufted cell networks in the mouse olfactory bulb. *Front Cell Neurosci* 15: 633757, 2021. doi:10.3389/fncel.2021.633757.
32. **Baker KL**, **Dickinson M**, **Findley TM**, **Gire DH**, **Louis M**, **Suver MP**, **Verhagen JV**, **Nagel KI**, **Smear MC.** Algorithms for olfactory search across species. *J Neurosci* 38: 9383–9389, 2018. doi:10.1523/JNEUROSCI.1668-18.2018.
33. **Dasgupta D**, **Warner TP**, **Erskine A**, **Schaefer AT.** Coupling of mouse olfactory bulb projection neurons to fluctuating odor pulses. *J Neurosci* 42: 4278–4296, 2022. doi:10.1523/JNEUROSCI.1422-21.2022.
34. **Ackels T**, **Erskine A**, **Dasgupta D**, **Marin AC**, **Warner TPA**, **Tootoonian S**, **Fukunaga I**, **Harris JJ**, **Schaefer AT.** Fast odour dynamics are encoded in the olfactory system and guide behaviour. *Nature* 593: 558–563, 2021. doi:10.1038/s41586-021-03514-2.
35. **Chong E**, **Moroni M**, **Wilson C**, **Shoham S**, **Panzeri S**, **Rinberg D.** Manipulating synthetic optogenetic odors reveals the coding logic of olfactory perception. *Science* 368: eaba2357, 2020. doi:10.1126/science.aba2357.
36. **Gumaste A**, **Coronas-Samano G**, **Hengenius J**, **Axman R**, **Connor EG**, **Baker KL**, **Ermentrout B**, **Crimaldi JP**, **Verhagen JV.** A comparison between mouse, in silico, and robot odor plume navigation reveals advantages of mouse odor tracking. *eNeuro* 7: ENEURO.0212-19.2019, 2020. doi:10.1523/ENEURO.0212-19.2019.
37. **Gire DH**, **Kapoor V**, **Arrighi-Allisan A**, **Seminara A**, **Murthy VN.** Mice develop efficient strategies for foraging and navigation using complex natural stimuli. *Curr Biol* 26: 1261–1273, 2016. doi:10.1016/j.cub.2016.03.040.
38. **Jordan R**, **Kollo M**, **Schaefer AT.** Sniffing Fast: paradoxical effects on odor concentration discrimination at the levels of olfactory bulb output and behavior. *eNeuro* 5: ENEURO.0148-18.2018, 2018. doi:10.1523/ENEURO.0148-18.2018.
39. **Wilson CD**, **Serrano GO**, **Koulakov AA**, **Rinberg D.** A primacy code for odor identity. *Nat Commun* 8: 1477, 2017. doi:10.1038/s41467-017-01432-4.
40. **Rolls ET**, **Treves A**, **Tovee MJ.** The representational capacity of the distributed encoding of information provided by populations of neurons in the primate temporal visual cortex. *Exp Brain Res* 114: 149–162, 1997. doi:10.1007/PL00005615.
41. **Franco L**, **Rolls ET**, **Aggelopoulos NC**, **Treves A.** The use of decoding to analyze the contribution to the information of the correlations between the firing of simultaneously recorded neurons. *Exp Brain Res* 155: 370–384, 2004. doi:10.1007/s00221-003-1737-5.
42. **Ratzlaff EH**, **Grinvald A.** A tandem-lens epifluorescence macroscope: hundred-fold brightness advantage for wide-field imaging. *J Neurosci Methods* 36: 127–137, 1991. doi:10.1016/0165-0270(91)90038-2.
43. **Lam YW**, **Cohen LB**, **Wachowiak M**, **Zochowski MR.** Odors elicit three different oscillations in the turtle olfactory bulb. *J Neurosci* 20: 749–762, 2000. doi:10.1523/JNEUROSCI.20-02-00749.2000.
44. **Wesson DW**, **Carey RM**, **Verhagen JV**, **Wachowiak M.** Rapid encoding and perception of novel odors in the rat. *PLOS Biol* 6: e82, 2008. doi:10.1371/journal.pbio.0060082.
45. **Carey RM**, **Verhagen JV**, **Wesson DW**, **Pírez N**, **Wachowiak M.** Temporal structure of receptor neuron input to the olfactory bulb imaged in behaving rats. *J Neurophysiol* 101: 1073–1088, 2009. doi:10.1152/jn.90902.2008.
46. **Cover TM**, **Thomas JA.** *Elements of Information Theory*. New York: Wiley, 1991.
47. **Treves A**, **Rolls ET.** A computational analysis of the role of the hippocampus in memory. *Hippocampus* 4: 374–391, 1994. doi:10.1002/hipo.450040319.
48. **Treves A**, **Rolls ET.** What determines the capacity of autoassociative memories in the brain? *Network* 2: 371–397, 1991. doi:10.1088/0954-898X_2_4_004.
49. **Rolls ET**, **Treves A.** The relative advantages of sparse versus distributed encoding for associative neuronal networks in the brain. *Network* 1: 407–421, 1990. doi:10.1088/0954-898X_1_4_002.
50. **Najac M**, **Sanz Diez A**, **Kumar A**, **Benito N**, **Charpak S**, **De Saint Jan D.** Intraglomerular lateral inhibition promotes spike timing variability in principal neurons of the olfactory bulb. *J Neurosci* 35: 4319–4331, 2015. doi:10.1523/JNEUROSCI.2181-14.2015.
51. **Phillips ME**, **Sachdev RN**, **Willhite DC**, **Shepherd GM.** Respiration drives network activity and modulates synaptic and circuit processing of lateral inhibition in the olfactory bulb. *J Neurosci* 32: 85–98, 2012. doi:10.1523/JNEUROSCI.4278-11.2012.

52. **Shepherd GM**, **Brayton RK.** Computer simulation of a dendrodendritic synaptic circuit for self- and lateral-inhibition in the olfactory bulb. *Brain Res* 175: 377–382, 1979. doi:10.1016/0006-8993(79)91020-5.
53. **Urban NN.** Lateral inhibition in the olfactory bulb and in olfaction. *Physiol Behav* 77: 607–612, 2002. doi:10.1016/s0031-9384(02)00895-8.
54. **Whitesell JD**, **Sorensen KA**, **Jarvie BC**, **Hentges ST**, **Schoppa NE.** Interglomerular lateral inhibition targeted on external tufted cells in the olfactory bulb. *J Neurosci* 33: 1552–1563, 2013. doi:10.1523/JNEUROSCI.3410-12.2013.
55. **Roper SD**, **Chaudhari N.** Taste buds: cells, signals and synapses. *Nat Rev Neurosci* 18: 485–497, 2017. doi:10.1038/nrn.2017.68.
56. **Rolls ET**, **Critchley HD**, **Verhagen JV**, **Kadohisa M.** The representation of information about taste and odor in the orbitofrontal cortex. *Chemosens Percept* 3: 16–33, 2010. doi:10.1007/s12078-009-9054-4.
57. **Johnson BA**, **Farahbod H**, **Leon M.** Interactions between odorant functional group and hydrocarbon structure influence activity in glomerular response modules in the rat olfactory bulb. *J Comp Neurol* 483: 205–216, 2005. doi:10.1002/cne.20409.
58. **Leon M**, **Johnson BA.** Olfactory coding in the mammalian olfactory bulb. *Brain Res Brain Res Rev* 42: 23–32, 2003. doi:10.1016/s0165-0173(03)00142-5.
59. **Sharp FR**, **Kauer JS**, **Shepherd GM.** Local sites of activity-related glucose metabolism in rat olfactory bulb during olfactory stimulation. *Brain Res* 98: 596–600, 1975. doi:10.1016/0006-8993(75)90377-7.
60. **Uchida N**, **Mainen ZF.** Speed and accuracy of olfactory discrimination in the rat. *Nat Neurosci* 6: 1224–1229, 2003. doi:10.1038/nn1142.
61. **Slotnick B**, **Restrepo D.** Olfactometry with mice. *Curr Protoc Neurosci* 2005: Unit 8.20, 2005. doi:10.1002/0471142301.ns0820s33.
62. **Verhagen JV**, **Wesson DW**, **Netoff TI**, **White JA**, **Wachowiak M.** Sniffing controls an adaptive filter of sensory input to the olfactory bulb. *Nat Neurosci* 10: 631–639, 2007. doi:10.1038/nn1892.
63. **Vincis R**, **Gschwend O**, **Bhaukaurally K**, **Beroud J**, **Carleton A.** Dense representation of natural odorants in the mouse olfactory bulb. *Nat Neurosci* 15: 537–539, 2012. doi:10.1038/nn.3057.
64. **Storace DA**, **Cohen LB.** Measuring the olfactory bulb input-output transformation reveals a contribution to the perception of odorant concentration invariance. *Nat Commun* 8: 81, 2017. doi:10.1038/s41467-017-00036-2.
65. **Tovée MJ**, **Rolls ET**, **Treves A**, **Bellis RP.** Information encoding and the responses of single neurons in the primate temporal visual cortex. *J Neurophysiol* 70: 640–654, 1993. doi:10.1152/jn.1993.70.2.640.
66. **Rolls ET**, **Aggelopoulos NC**, **Franco L**, **Treves A.** Information encoding in the inferior temporal cortex: contributions of the firing rates and correlations between the firing of neurons. *Biol Cybern* 90: 19–32, 2004. doi:10.1007/s00422-003-0451-5.
67. **Panzeri S**, **Schultz SR**, **Treves A**, **Rolls ET.** Correlations and the encoding of information in the nervous system. *Proc Biol Sci* 266: 1001–1012, 1999. doi:10.1098/rspb.1999.0736.
68. **Panzeri S**, **Biella G**, **Rolls ET**, **Skaggs WE**, **Treves A.** Speed, noise, information and the graded nature of neuronal responses. *Network* 7: 365–370, 1996. doi:10.1088/0954-898X/7/2/018.
69. **Rebello MR**, **Kandukuru P**, **Verhagen JV.** Direct behavioral and neurophysiological evidence for retronasal olfaction in mice. *PLoS One* 10: e0117218, 2015. doi:10.1371/journal.pone.0117218.
70. **Rolls ET**, **Critchley HD**, **Treves A.** The representation of olfactory information in the primate orbitofrontal cortex. *J Neurophysiol* 75: 1982–1996, 1996. doi:10.1152/jn.1996.75.5.1982.
71. **Rolls ET**, **Critchley HD**, **Mason R**, **Wakeman EA.** Orbitofrontal cortex neurons: role in olfactory and visual association learning. *J Neurophysiol* 75: 1970–1981, 1996. doi:10.1152/jn.1996.75.5.1970.
72. **Critchley HD**, **Rolls ET.** Olfactory neuronal responses in the primate orbitofrontal cortex: analysis in an olfactory discrimination task. *J Neurophysiol* 75: 1659–1672, 1996. doi:10.1152/jn.1996.75.4.1659.
73. **Rolls ET**, **Treves A**, **Tovee MJ**, **Panzeri S.** Information in the neuronal representation of individual stimuli in the primate temporal visual cortex. *J Comput Neurosci* 4: 309–333, 1997. doi:10.1023/a:1008899916425.
74. **Tovee MJ**, **Rolls ET.** Information encoding in short firing rate epochs by single neurons in the primate temporal visual cortex. *Vis Cogn* 2: 35–58, 1995. doi:10.1080/13506289508401721.
75. **Rolls ET**, **Tovee MJ.** Processing speed in the cerebral cortex and the neurophysiology of visual masking. *Proc Biol Sci* 257: 9–15, 1994. doi:10.1098/rspb.1994.0087.
76. **Critchley HD**, **Rolls ET.** Olfactory neuronal responses in the primate orbitofrontal cortex: analysis in an olfactory discrimination task. *J Neurophysiol* 75: 1659–1672, 1996. doi:10.1152/jn.1996.75.4.1659.
77. **Courtiol E**, **Wilson DA.** The olfactory mosaic: bringing an olfactory network together for odor perception. *Perception* 46: 320–332, 2017. doi:10.1177/0301006616663216.
78. **Wilson DA**, **Chapuis J**, **Sullivan RM.** Cortical olfactory anatomy and physiology. In: *Handbook of Olfaction and Gustation*, edited by Doty RL. Hoboken, NJ: Wiley, 2015, p. 209–223.
79. **Franco L**, **Rolls ET**, **Aggelopoulos NC**, **Jerez JM.** Neuronal selectivity, population sparseness, and ergodicity in the inferior temporal visual cortex. *Biol Cybern* 96: 547–560, 2007. doi:10.1007/s00422-007-0149-1.